Minimization of Vibration and Acoustic Noise in Flux-Switching Permanent-Magnet Motors Based on Double Fault-Tolerant Teeth

Zheng Wang[1], Guohai Liu[2], Yanxin Mao[1], and Liang Xu[1]
[1]School of Electrical and Information Engineering, Jiangsu University, Zhenjiang 212013, China
[2]Jiangsu Key Laboratory of Drive and Intelligent Control for Electric Vehicle, Zhenjiang212013, China
Email: 1357989734@qq.com

***Abstract*—Flux-switching permanent-magnet (FSPM) motors are been studied as a promising candidate for many industrial applications, but they suffer from vibration and acoustic noise of electromagnetic origins. This paper proposes a new five-phase fault-tolerant FSPM motor in order to reduce vibration and acoustic noise, which has double fault-tolerant teeth on stator. By cutting down the lowest harmonic of radial force density, vibration and acoustic noise characteristics of the proposed motor is improved. Results indicate that the proposed motor retains the merits of existing FSPM motors, and offers less vibration, smaller acoustic noise.**

Keywords—Flux-switching permanent-magnet motors, radial force density, cogging torque, vibration, acoustic noise

I. INTRODUCTION

Flux switching motors were firstly proposed as a single phase permanent-magnet (PM) [1] and re-emerged as five-phase 10/18 stator/rotor pole flux-switching PM (FSPM) motors due to high reliability and high efficiency [2]-[4]. Recently, new fault-tolerant FSPM (FT-FSPM) motor topologies, in which each phase is magnetically and physically isolated, have been proposed [5]-[8]. However, it still suffers from severe asymmetry in flux linkage and hence back electromotive force (EMF) waveforms, thus causing serious torque ripples which lead to vibration and acoustic noise. Even with the use of rotor skewing to enhance more sinusoidal back-EMF at the cost of reducing the voltage amplitude, the problem of asymmetry can not be solved. Also, FSPM motors usually have high local magnetic stress. Numerical simulations and experimental tests verified that vibration and acoustic noise in FSPM motor should be considered as a critical issue. The former research on vibration and acoustic noise has been focused on different types of electric motors, such as switched reluctance motors and fractional slot concentrated winding surface PM motors [9]-[12]. It has been not reported that by using topology and design technique to minimize the vibration and acoustic noise in FSPM motors.

The electromagnetic vibration sources include cogging torque, torque ripple and radial force, etc. [13]. The radial vibration force distribution on the stator bore is the main cause of electromagnetically induced vibration and acoustic noise at no-load and at load conditions [14]. The lowest harmonic of radial force leads to huge vibration, therefore, by reducing lowest harmonic of radial force at the design stage, a consideration reduction in the vibration and acoustic noises can be aimed at.

The purpose of this paper is to propose and design a new five-phase FSPM motor which has double fault-tolerant teeth (FTT) on stator. This topology can not only retain the advantages of the existing fault-tolerant FSPM (FT-FSPM) motors and the multiphase motors, but also minimize the vibration and acoustic noise of the existing FT-FSPM motors. With the use of finite element method (FEM), the influences of the different stator core of the newly designed FSPM motors will be investigated, including cogging torque, back-EMF, torque, inductance, radial force density, vibration and acoustic noise.

II. MOTOR TOPOLOGIES AND SPECIFICATIONS

Fig. 1 shows the cross-section of the existing and the proposed FT-FSPM motors. Both motors have very simple rotors, similar to that of a switched reluctance motor, which both magnets and coils located in the stator. It can be seen that the proposed FT-FSPM motor has double FTT on the stator which obviously differs from the conventional topology. Width of FTT of the proposed FT-FSPM motor is a half of the original one, and the spacing between the double FTT of the proposed FT-FSPM motor equals the width of FTT of existing FT-FSPM motor. Since the multi-teeth structure of stator is adopted, cogging torque of proposed FT-FSPM motor can be reduced. For a fair comparison, both motors designed in this work are targeted at the specification detailed in Table I.

III. ELECTROMAGNETIC PERFORMANCE ANALYSIS

By using FEM, two topologies will be compared based on cogging torque, back-EMF, torque, inductance, and harmonic of radial force density.

A. Cogging Torque

cogging torque waveforms of both FSPM motors are compared in Fig. 2. The proposed topology can offer less cogging torque than the existing one, namely, the proposed FT-FSPM motor can minimize 38% cogging torque than the existing FT-FSPM motor because of the multi-teeth structure on stator. Cogging torque does not contribute to output torque, only results in pulsations which represent undesirable vibration and acoustic noise.

978-1-5090-3528-1/16/$31.00 ©2016 IEEE

B. *Back-EMF*

When the FT-FSPM motors operate at the rated speed of 1500 r/min, their no-load back-EMFs are shown in Fig. 3. It can be found that the both FT-FSPM motors have practically the same peak-to-peak value of back-EMFs. Obviously, the proposed FT-FSPM motor has a much more sinusoidal and symmetric back-EMF waveform than the existing one. Namely, the positive and negative peak value of the back-EMF waveform of the proposed FT-FSPM motor are 141 V and 152V, respectively, whereas those values of the existing one are 153 V and -134 V, respectively. By applying spectral analysis to the back-EMF waveform, the corresponding fundamental components and harmonics can be deduced as shown in Fig. 4. It can be observed that the existing FT-FSPM motor exhibits much more serious harmonic distortion than the proposed one. Quantitatively, the total harmonic distortion of the back-EMF waveform of the existing FT-FSPM motor is 9.1% which higher than the 7.6% of the proposed one.

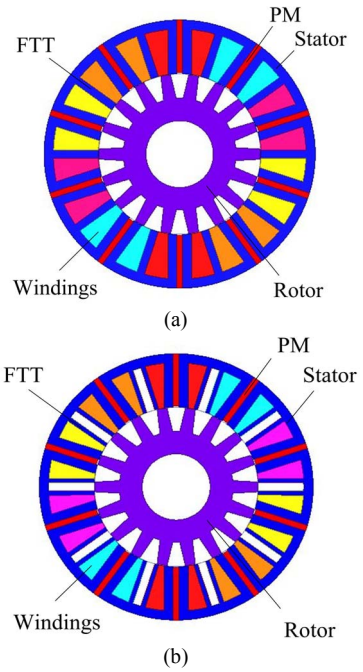

Fig. 1. Cross-section of the FT-FSPM motors. (a) Existing. (b) Proposed.

TABLE I. MOTORS SPECIFICATIONS

Parameters	Existing motor	Proposed motor
Rated current (A)	10	10
Rated speed (r/min)	1500	1500
Stator outer radius (mm)	72.5	72.5
Stator inner radius (mm)	43.5	43.5
Airgap length (mm)	0.4	0.4
Axial length (mm)	60	60
Turns per coil	70	70
Rotor poles	18	18
Stator poles	10	10
FTT width (mm)	4.4	2.2

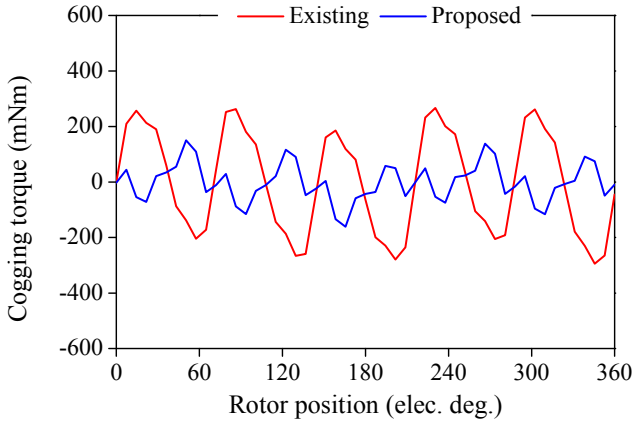

Fig. 2. Comparison of cogging torque waveforms.

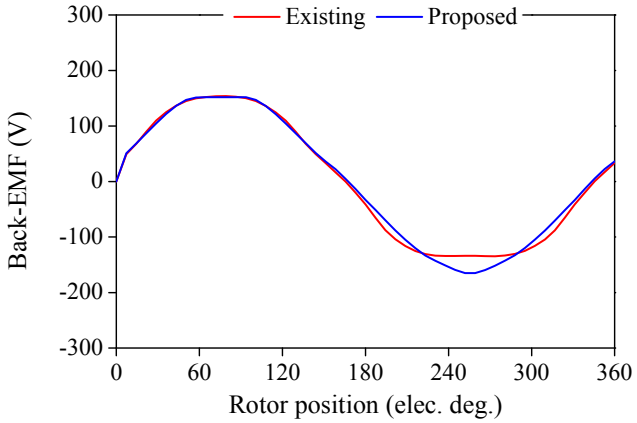

Fig. 3. Comparison of back-EMF waveforms.

C. *Torque*

Fig. 5 shows the output torque of both FT-FSPM motors, which are at the same rated current of 10 A. The average torque of proposed FT-FSPM motors is decreased from 27.1 Nm to 26.1 Nm compared with the existing FSPM motors. The torque ripple ratio K_T defined as:

$$K_T = \frac{T_{\max} - T_{\min}}{T_{avg}} \quad (1)$$

where T_{max} T_{min}, and T_{avg} are the maximum, minimum and average values of cogging torque, respectively. By defining the torque ripple factor as the percentage ratio of peak-to-peak torque to average torque, it can be seen that the torque ripple of proposed FT-FSPM motor is much better than the existing one.

D. *Inductance*

The corresponding self inductance and mutual inductance are calculated. Table III lists inductances of the proposed FT-

FSPM motor as compared with those of the existing FT-FSPM motor. It can be found that the ratio of mutual inductance to self inductance of the existing FT-FSPM motor is larger than that of the proposed double FTT motor, indicating that the existing one exhibits closely coupled phases while the proposed FT-FSPM motor are essentially phase decoupling.

E. Harmonic of Radial Force Density

The radial force density at the airgap can be expressed as fr, which can be calculated by,

$$f_r = \frac{B_r^2 - B_t^2}{2\mu_0} \tag{2}$$

where μ_0 is the permeability of the free space, B_r is the magnetic flux density in the normal direction, B_t is the magnetic flux density in the tangential direction. Fig. 6 shows that radial force density harmonics of two motors. The lowest harmonic order has dominant influence on vibration and acoustic noise. Radial force density will attain a large value when motor stator pole alignment rotor pole, the double FTT structure leads the distribution of radial force density more symmetrical. As shown in Fig. 6, the new structure of FT-FSPM can significantly cut down the 2nd harmonic component.

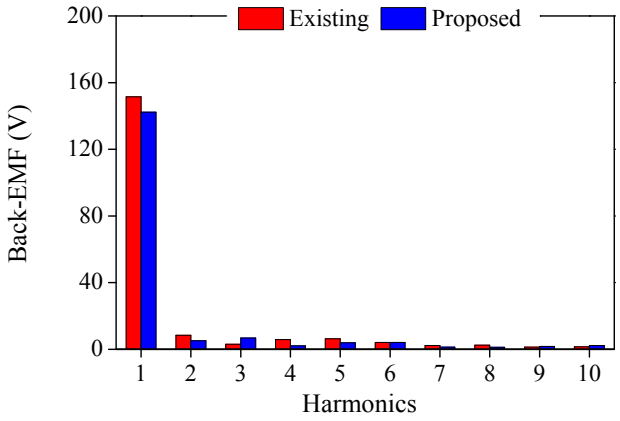

Fig. 4. Comparison of back-EMF harmonics.

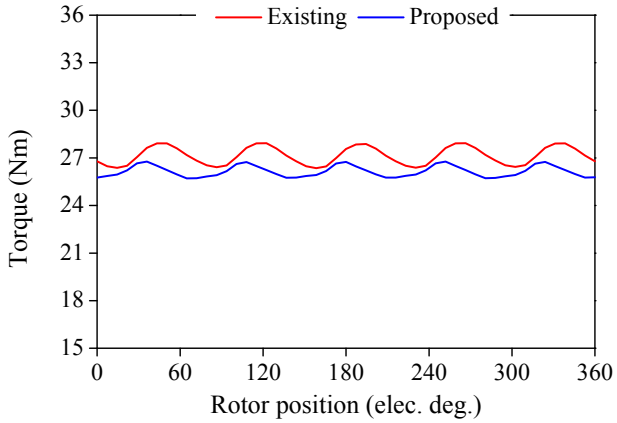

Fig. 5. Comparison of torque waveforms at rated current.

TABLE II. AVERAGE TORQUE AND TORQUE RIPPLE RATIO

Parameters	Existing motor	Proposed motor
Rated average torque (Nm)	27.1	26.1
K_T (%)	5.8	4.1

TABLE III. COMPARISON OF SELF AND MUTUAL INDUCTANCES

	L (mH)	M (mH)	M/L (%)
Existing motor	7.81	1.27	16.26
Proposed motor	7.53	0.96	12.75

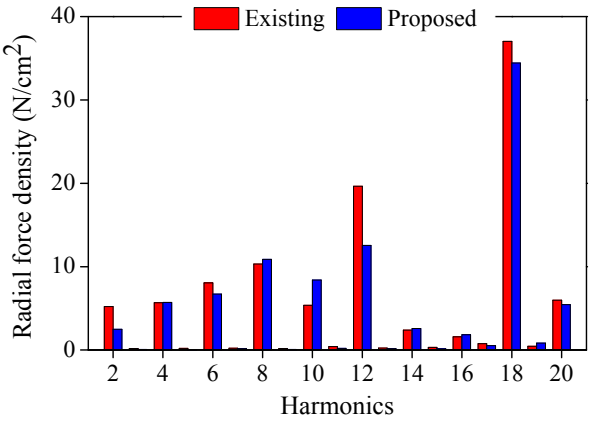

Fig. 6. Harmonics of radial force density

IV. VIBRATION AND NOISE

The electromagnetic force of existing and proposed FSPM motors at the same rated current 10A is calculated in Fig. 7. It should be noted that the teeth of stator suffer from lager electromagnetic force than stator yoke. After importing the electromagnetic force which the stator is received into the LMS Virtual Lab, the expanded structural response from natural modes can be computed. Fig. 8 shows that the teeth of stator have evident deformation on two motors. It can be seen that structural response of proposed FT-FSPM motor has less vibration than the existing one at 1500 Hz. The maximum displacement of existing FT-FSPM motor is about 1.2×10-3 mm and the proposed FT-FSPM motor is about 7.2×10-4 mm. Large vibration will damage the motor structure, lead to loud acoustic noise. The proposed FT-FSPM motor can restrain vibration on stator as expected.

Once the structural response is obtained for the whole frequency range of interest, the structural response can be used as the boundary condition for acoustic model to calculate acoustic noise. In this section, LMS Virtual Lab is used to perform this task to generate acoustic noise. The result shows in Fig. 9(a), which indicated the acoustic pressure of the existing FT-FSPM motor on circular surface of the measurement field is around 62 dB at 1500 Hz, the acoustic pressure of the proposed FT-FSPM motor is around 50 dB at the same frequency in Fig.

9(b). The proposed FT-FSPM motor can effectively minimize sound pressure amplitude.

Sound power level of the existing FT-FSPM motor and the proposed FT-FSPM motor are shown in Fig. 10 in the range [100 Hz; 5600 Hz]. As shown in Fig. 10, the proposed FT-FSPM motor can significantly reduce the acoustic noise at 1500 Hz and 4300 Hz. When new stator structure is adopted, the total acoustic power of existing FT-FSPM motor descends from 73.4 dB to 68.1 dB. The proposed FT-FSPM motor can availably minimize acoustic noise power about 66%.

V. Conclusion

This paper has proposed a new double FTT FSPM motor which contributes to the minimization of vibration and acoustic noise. Its electromagnetic performance has been analyzed as compared with the existing FT-FSPM motor. It has demonstrated that the proposed motor can greatly reduce cogging torque, provide sinusoidal back-EMF, subsequently, minimize vibration and acoustic noise. The torque characteristics show that the torque of proposed topology is slightly smaller than the existing FT-FSPM motor, however, the torque ripple is reduced greatly. The proposed FT-FSPM motor can lead to less vibration and acoustic noise than existing FT-FSPM motor, because it make the distribution of radial force density more symmetrical. The double FTT FSPM motor provides desirable for reducing vibration and acoustic noise.

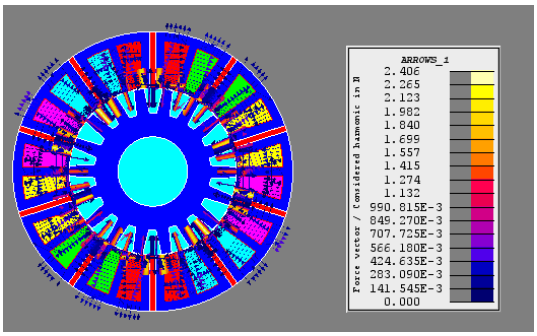

(a)

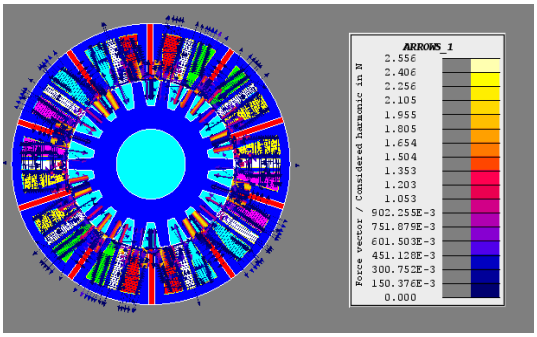

(b)

Fig. 7. Stator core force. (a) Existing FT-FSPM motor. (b) Proposed FT-FSPM motor.

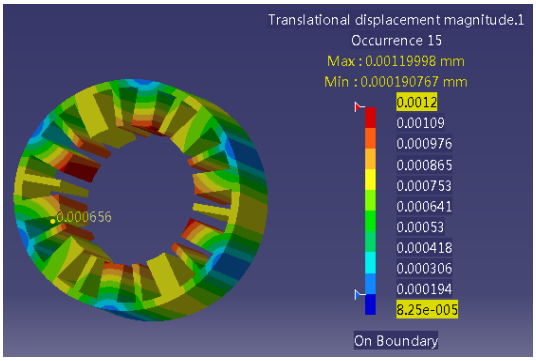

(a)

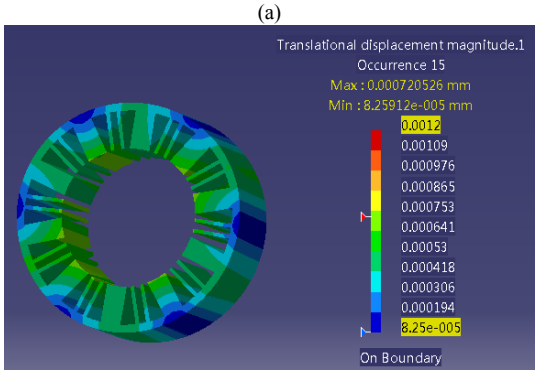

(b)

Fig. 8. Stator core deformation. (a) Existing FT-FSPM motor. (b) Proposed FT-FSPM motor.

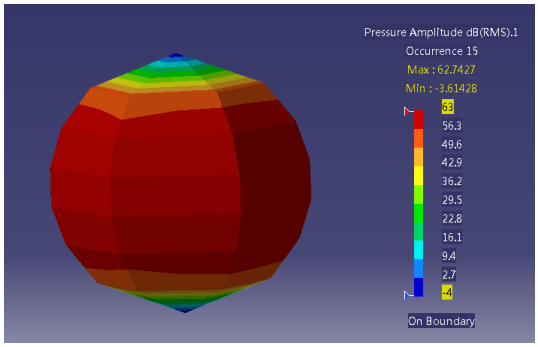

(a)

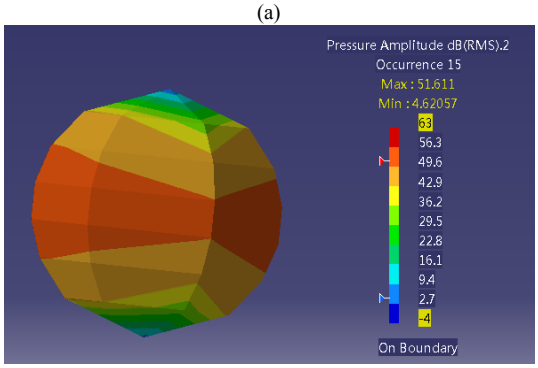

(b)

Fig. 9. Acoustic noise image at 1500 Hz. (a) Existing FT-FSPM motor. (b) Proposed FT-FSPM motor.

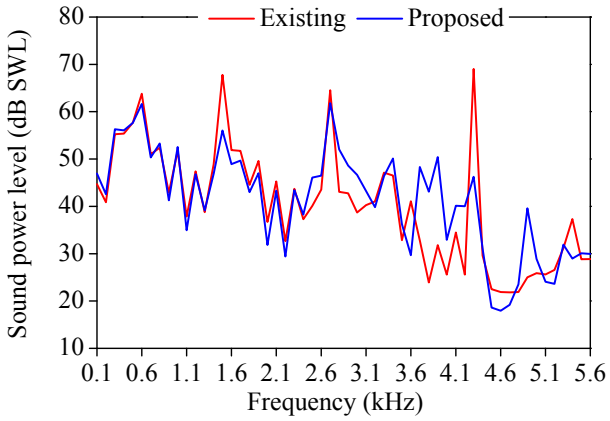

Fig. 10. Sound power levels of load configuration in range [100 Hz; 5600 Hz]

ACKNOWLEDGMENT

This work was supported by the National Natural Science Foundation of China (61273154 and 51577084), by the Research Fund for 333 Project of Jiangsu Province (Project BRA2015302), by the Key Project of Natural Science Foundation of Jiangsu Higher Education Institutions (15KJA470002), and by the Priority Academic Program Development of Jiangsu Higher Education Institutions.

REFERENCES

[1]. S. E. Rauch, and L. J. Johnson, "Design principles of the flux-switch alternators," AIEE Trans., vol. 74, no. 3, pp. 1261-1268, Jan. 1955.

[2]. X. Xue, W. Zhao, J. Zhu, G. Liu, X. Zhu, and M. Cheng, "Design of five-phase modular flux-switching permanent-magnet machines for high reliability applications," IEEE Trans. Magn., vol. 49, no. 7, pp. 3941-3944, Jul. 2013.

[3]. J. Boisson, F. Louf, J. Ojeda, X. Mininger, and M. Gabsi, "Low computational-cost determination of vibrational behavior: application to five-phase flux-switching permanent-magnet motor," IEEE Trans. Magn., DOI: 10.1109/TMAG.2014.2359952, 2014.

[4]. J. T. Chen, Z. Q. Zhu, S. Iwasaki and Rajesh P. Deodhar, "Influence of slot opening on optimal stator and rotor pole combination and electromagnetic performance of switched-flux PM brushless AC machines," IEEE Trans. Ind. Appl., vol. 47, no. 4, pp. 1681-1691, July/Aug. 2011.

[5]. W. Zhao, M. Cheng, K. T. Chau, and C. C. Chau, "Control and operation of fault-tolerant flux-switching permanent-magnet motor drive with second harmonic current injection," IET Electric Power Appl., vol. 6, no. 9, pp. 707-715, Aug. 2012.

[6]. W. Zhao, M. Cheng, K. T. Chau, J. Ji, and R. Cao, "Remedial injected harmonic current operation of redundant flux-switching permanent magnet motor drives," IEEE Trans. Ind. Electron., vol. 60, no. 1, pp. 151-159, Jan. 2013.

[7]. W. Zhao, M. Cheng, W. Hua, H. Jia, and R. Cao "Back-EMF harmonic analysis and fault-tolerant control of flux-switching permanent-magnet machine with redundancy," IEEE Trans. Ind. Electron., vol. 58, no. 5, pp. 1926-1936, May 2011.

[8]. W. Zhao, M. Cheng, K. Chau, W. Hua, H. Jia, J. Ji, and W. Li, "Stator-flux-oriented fault-tolerant control of flux-switching permanent-magnet motors," IEEE Trans. Magn., vol. 47, no. 10, pp. 4191-4194, Oct. 2011.

[9]. C. Gan, J. Wu, M. Shen, S. Yang, Y. Hu, and W. Cao "Investigation of skewing effects on the vibration reduction of three-phase switched reluctance motors," IEEE Trans. Magn., vol. 51, no. 9, Nov. 2014, Art. ID. 8203509.

[10]. A. Isfahani and B. Fahimi, "Comparison of mechanical vibration between a double-stator switched reluctance machine and a conventional switched reluctance machine," IEEE Trans. Magn., vol. 50, no. 2, Feb. 2014, Art. ID. 7007104.

[11]. D. Dorrell, M. Popescu, and D. Ionel, "Magnetic pull due to asymmetry and low-level static rotor eccentricity in fractional-slot brushless permanent-magnet motors with surface-magnet and consequent-pole," IEEE Trans. Magn., vol. 46, no. 7, pp. 2675-2685, Mar. 2010.

[12]. M. Islam, R. Islam, and T. Sebastian, "Noise and vibration characteristics of permanent-magnet synchronous motors using electromagnetic and structural analyses," IEEE Trans. Ind. Appl., vol. 50, no. 5, pp. 3214-3222, Sep. 2014.

[13]. H. J. Shin, J. Y. Choi, H. I. Park, and S. M. Jang, "Vibration analysis and measurements through prediction of electromagnetic vibration sources of permanent magnet synchronous motor based on analytical magnetic field calculations," IEEE Trans. Magn., vol. 48, no. 11, pp. 4216-4219, Nov. 2012.

[14]. G. Dajaku and D. Gerling, "The influence of permeance effect on the magnetic radial forces of PM synchronous machines," IEEE Trans. Magn., vol. 49, no. 6, pp. 2953-2966, Jan. 2013